Geoderma 263 (2016) 195–202

Contents lists available at ScienceDirect

Geoderma

journal homepage: www.elsevier.com/locate/geoderma

Laser-induced breakdown spectroscopy to determine soil texture: A fast analytical technique

Paulino Ribeiro Villas-Boas [a,*], Renan Arnon Romano [a,b], Marco Aurélio de Menezes Franco [a,c], Edilene Cristina Ferreira [d], Ednaldo José Ferreira [a], Silvio Crestana [a], Débora Marcondes Bastos Pereira Milori [a]

[a] Embrapa Instrumentation, R. XV de Novembro, 1452, 13560–970 São Carlos, SP, Brazil
[b] Physics Institute of São Carlos, University of São Paulo, IFSC-USP, Av. Trabalhador Sancarlense, 400 Pq. Arnold Schimid, 13566–590 São Carlos, SP, Brazil
[c] Physics Department, São Carlos Federal University, P.O. Box 676, 13565–905 São Carlos, SP, Brazil
[d] São Paulo State University — UNESP, Analytical Chemistry Department, P.O. Box 355, 14801–970, R. Prof. Francisco Degni, 55, 14800–900 Araraquara, SP, Brazil

ARTICLE INFO

Article history:
Received 17 July 2015
Received in revised form 17 September 2015
Accepted 20 September 2015
Available online 1 October 2015

Keywords:
Soil texture
Soil particle size
LIBS
Spectroscopy
PLSR

ABSTRACT

The analysis of soil texture is crucial for the proper management of agricultural systems and for environmental studies. Soil texture is important as it affects erosion potential, water retention capacity, organic matter complexation, and the retention of nutrients, among others. It is usually determined by pipette or hydrometer methods, but analysis requires a preparation with chemical reagents, which can take hours and hence is unfeasible for large number of samples. Here we propose the use of laser-induced breakdown spectroscopy (LIBS) to estimate the proportions of sand, silt, and clay in 60 Brazilian soil samples of varying composition. Two calibration models were developed with the partial least square regression method: one considering the spectral region from 188 to 980 nm and the other, emission lines of the elements Si, Na, Fe, Ti, Ca, K, Al, Co, Mg, V, Ba, and Be. The Pearson correlation coefficients for the estimated values were 0.89 and 0.90 on average for the first and second models, respectively. The uncertainties were 6% on average for both models. These results demonstrate the use of LIBS for rapid scanning of the texture of soil samples with distinct composition. The procedure presented here can be extended to other chemical and physical soil properties, which makes LIBS a universal tool for rapid soil analysis without preparation with chemical reagents.

1. Introduction

The relative proportion of sand, silt, and clay – texture – is one of the most important physical properties of soils. It directly affects other critical properties, including susceptibility to erosion, drainage, water-holding capacity, organic matter content, and capacity for leaching nutrients and pollutants (Hassink et al., 1993). Soil texture is, therefore, one of the key components for assessing soil quality and the sustainability of agricultural management practices (Kettler et al., 2001).

In the field, agronomists can estimate soil texture by rubbing a soil sample between their fingers and thumb and feeling its physical characteristics. However, such a technique is of low accuracy and requires skill and experience (Brown, 2003). In the laboratory, sand can be easily separated from soil samples by sieving, and clay and silt can be accurately determined by two well-established conventional methods: pipette and hydrometer. The former is more accurate and is considered the standard method for texture determination. It is based on Stoke's law, which states that denser (i.e. larger) particles sink faster than lighter (i.e. smaller) particles. Therefore, after a predetermined time in water suspension clay particles can be separated from the settled silt. Despite its accuracy, the pipette method is time-consuming and laborious, depends on the operator and requires sample pretreatment to disperse soil aggregates (Gee and Bauder, 1986; Kettler et al., 2001).

Other methods for direct determination of soil particle sizes have been developed, including gamma-ray attenuation (Naime et al., 2001), X-ray attenuation, electroresistance particle counting, photometrical techniques, and laser diffractometry (e.g., McCave and Syvitski, 2007). Prior to analysis, however, all these methods also require a pre-processing step to disperse the aggregates, which usually takes a full day. Furthermore, these methods do not have proper correspondence with the pipette or hydrometer for determining the size of the smallest particles, clay and silt (Taubner et al., 2009). Soil texture can also be indirectly determined by visible or infrared reflectance spectroscopy (e.g., Chang et al., 2001; Madari et al., 2006; Rossel et al., 2006; Curcio et al., 2013). The reflectance spectroscopy does not require the sample pre-processing step and has a good correspondence with traditional methods, but its accuracy depends on the amount and diversity of samples used to build calibration models.

In this article, we propose a method for evaluating the relative proportions of sand, clay, and silt in soils without the need for preparing samples, hence reducing the overall time of analysis to a few minutes.

* Corresponding author.
E-mail address: paulino.villas-boas@embrapa.br (P.R. Villas-Boas).

http://dx.doi.org/10.1016/j.geoderma.2015.09.018
0016-7061/

The method consists in using the soil elemental composition assessed by laser-induced breakdown spectroscopy (LIBS) (Miziolek et al., 2006) and building calibration models based on the correlation between emission lines and the relative proportions of sand, silt, and clay. We hypothesized that each relative proportion is mainly constituted by certain elements (e.g., silicon in sand), which are either absent or present in small amounts in the other proportions.

The LIBS is a multi-elemental spectroscopic technique based on emission of plasma induced by laser (Miziolek et al., 2006; Cremers and Radziemski, 2006; Singh and Thakur, 2007). Sample can be analyzed with minimal manipulation (i.e. without reagents) or even directly in situ (Theriault et al., 1998; Harmon et al., 2005; Corsi et al., 2006; Palanco et al., 2006). The LIBS analytic process starts by focusing a highly energetic pulse onto the sample. The laser energy density is so high ($\sim 10^9$ W cm^{-2}) that it can break molecular bonds, generating a small plasma plume — a gas of unbound atoms, ions, electrons, and photons. During laser interaction, the ablated material can reach a temperature of 100,000 K (Miziolek et al., 2006), whereby its emission is basically composed of continuum radiation. As the plasma cools, the continuum emission reduces, allowing the observation of atomic and ionic lines derived from the excited elements (Singh and Thakur, 2007), which is usually performed at ~10,000 K. The elemental composition of the samples can be determined, and with appropriate calibration models the elemental concentration can be obtained. In the case of soil analysis, the LIBS has been applied to evaluate nutrients (Hussain et al., 2007; Ferreira et al., 2011; Braga et al., 2010; Cremers et al., 2001; Ebinger et al., 2003), contaminants (Bousquet et al., 2007; Senesi et al., 2009), and carbon (Nicolodelli et al., 2014; Ebinger and Harris, 2010; Silva et al., 2008), as well as humification degree of soil organic matter (Ferreira et al., 2014), soil pH (Ferreira et al., 2015), and soil classification (Pontes et al., 2009). However, no applications of LIBS have been reported for the evaluation of any soil physical characteristics.

2. Materials and methods

2.1. Soil samples

A set of 60 samples, collected from farmlands all over Brazil and characterized by the Agronomic Institute of Campinas, São Paulo State, Brazil were used in the following analyses. The relative proportions of sand, silt, and clay were determined by the pipette method and were in the range of 4–92%, 2–35% and 6–66%, respectively. Prior to the texture analysis by the LIBS technique, the soil samples were sieved to remove roots and ground to reduce particle size heterogeneity by a cryogenic mill working with liquid nitrogen at a temperature of −196 °C. For the LIBS analysis, the ground samples were pressed into pellets with 10 tons of hand press.

2.2. Laser-induced breakdown spectroscopy (LIBS)

The LIBS spectra of the soil samples were acquired with a LIBS2500plus spectrometer (Ocean Optics, Dunedin, FL, USA), which utilized a Q-switched Nd:YAG laser at 1064 nm (Quantel, Bozeman, MT, USA) operating at 75 mJ maximum power energy, 8 ns pulse width, and 10 Hz frame rate. The laser pulse was focused on the sample inside an ablation chamber. After the plasma was formed, the emission of excited species was carried by an optical fiber bundle connected to seven spectrometers ranging from 188 to 980 nm, each one coupled with a 2048 element linear silicon CCD array whose resolution was ~0.1 nm (FWHM). The distance from the sample to the collecting optical fiber bundle was approximately 7 mm. All measurements were performed in air, and the LIBS system was set to 50 mJ per laser pulse with a 2.1 ms integration time and a fixed delay time of 2 μs. On each soil sample, 60 measurements were carried out, two accumulated shots each.

2.3. Spectral processing

The LIBS spectra of a sample may vary from one shot to another, since they are strongly affected by acquisition system and plasma instability. The former depends on optical and electronic systems and may impose offset and random noise on the spectra acquired. The latter is caused by several aspects related to radiation–matter interaction – also known as matrix effects – including the composition and aggregation state of the samples, surface roughness, homogeneity, and optical alignment. The plasma formation involves a combination of non-linear dynamics such as radiation–matter interaction, laser-ablation mechanisms, production of free electrons, radiation absorbed by the plasma, and reabsorption of the species (Tognoni et al., 2010). Also, because of the non-linear plasma formation, LIBS measurements follow a generalized distribution of extreme values (Michel and Chave, 2007), instead of a normal distribution. All these issues lead to a non-reproducible background continuum emission of the spectra, which makes quantitative elemental analysis difficult. To develop calibration models for elemental quantification with LIBS, these issues have to be eliminated or reduced. In this study, only offset, random noise, and background continuum emission were corrected.

The offset of each spectrum was corrected separately for each spectrometer by subtracting the minimum value found in each spectral region. To reduce the random noise, the spectra were smoothed with a Savitzky–Golay filter (Savitzky and Golay, 1964), whose parameters were selected according to the genetic optimization algorithm (Mebane and Sekhon, 2011).

The background continuum emission – the spectral baseline – was corrected by two methods. The first one was 4S Peak Filling (Liland, 2015), which was developed for similar spectra found in other spectroscopy techniques, such as NMR and Raman (Liland et al., 2010; Liland and Mevik, 2011). The method estimates the baseline by iteratively suppressing the spectrum with a moving window and is based on four operations: smoothing, subsampling, suppression, and stretching. The parameters of the 4S Peak Filling method were also selected according to the genetic optimization algorithm. The second method estimates a baseline for each peak independently through a linear fit of the points on the left and right sides. It depends on the fact that the baseline approaches a straight line for small spectral regions and considers only spectral points not belonging to peaks (Dawson et al., 1993).

Since finding the elements whose concentration was most correlated to the soil, textural proportions was also important for this study, the intensity of lines was approximated by the area of the fitted function to the experimental points. If the line of interest was interfered by other lines, a deconvolution method was applied, in which a distribution was fitted for each peak in the analyzed range. In this study, only Lorentzian distribution was considered for the peaks.

2.4. Calibration model

Since the sum of the relative proportions of sand, silt, and clay is 100%, it is not necessary to build a calibration model for all relative proportions. For instance, if a model is built to predict the relative proportion of sand and clay, the proportion of silt would be 100% minus the sum of the other two. However, the uncertainty of estimating the relative proportion of silt would be higher than if it was directly predicted by the model (assuming that the model is less accurate than the reference method). One way to improve the predictions using just two variables is to combine the relative proportions of sand, silt, and clay prior to building the calibration model. Thus, we defined two variables as follows:

$$\begin{aligned} e &= a - b - c \\ f &= b - c, \end{aligned} \tag{1}$$

where a, b and c are the relative proportions of sand, clay, and silt, respectively. Such a combination is similar to what is provided by

the pipette method, where sand is first separated from clay and silt by sieving, and then silt is separated from clay by sedimentation in an aqueous solution. After the model is built with variables *e* and *f*, the relative proportions of sand, clay, and silt can be obtained by the following expressions:

$$\begin{aligned} a &= (1+e)/2 \\ b &= (1+2f-e)/4 \\ c &= (1-2f-e)/4. \end{aligned} \quad (2)$$

A test (not shown) was performed to verify these assumptions, and the accuracy and precision of the model built with variables *e* and *f* were higher than those of the model built with *a*, *b*, and *c* or the model built with *a* and *b*, in which $c = 1 - a - b$. Therefore, the models were built with variables *e* and *f*.

Partial least square regression (PLSR) was the calibration model applied to correlate LIBS spectra with the variables *e* and *f*. PLSR is a multivariate linear statistical method, which finds the best combination of prediction variables to explain the variation in the response variable (e.g., Wold et al., 2001). To some extent, this method is similar to principal component analysis (PCA), which defines a new set of linearly independent variables ordered by maximum variance without relation to the response variables (e.g., Costa and Cesar, 2001). PLSR, on the other hand, determines a new set of variables whose variation is maximized to explain the response variables. This method is particularly useful when the number of prediction variables is higher than the number of observations, and the prediction variables are multicollinear (Tobias, 1995). The method is commonly used in chemometrics to quantify the concentration of elements in samples by considering their spectra. In this kind of application, PLSR is a suitable method since the number of spectral points is usually higher than the number of samples, and the transition lines are generally correlated among them. The model accuracy was evaluated by leave-one-out cross-validation, which consists in using all samples minus one to build the PLSR model and estimating the proportions of sand, clay, and silt with the remaining sample. The procedure is repeated until all samples are tested.

2.5. Data analysis

The overall data analysis involved several steps from spectral processing to the building of regression models, as schematized in Fig. 1. The analysis started by removing the offset and proceeded by dividing the 60 samples into two sets: one-quarter for spectral processing (optimization of spectral correction parameters and peak-finding) and the remainder for building the regression models. To be representative, the first set was chosen in such a way as to cover all types of textures ranging from clay to sandy soils uniformly distributed.

The second step in the data analysis was the spectral processing and peak-finding, represented by the left dotted block in Fig. 1. The spectral processing consisted in optimizing two methods: the Savitzky–Golay filter and 4S Peak Filling for random noise and baseline correction, respectively. Both methods were optimized with a genetic algorithm based on derivatives (Mebane and Sekhon, 2011), implemented in package rgenoud of the R programming environment (R Core Team, 2014). For each realization, random parameters were chosen according to the genetic algorithm for the methods to correct the spectra of the samples. Since each sample corresponded to 60 spectra, they were averaged after the corrections. The resulting spectra were then used to build a regression model for the variables *e* and *f* (Eq. (1)) with the PLSR model and tested with leave-one-out cross-validation. The result of each realization was $\overline{\rho}$: the average of correlation coefficients calculated between the estimated and measured soil textural proportions. The estimated proportions were obtained according to Eq. (2). The optimization procedure finished when the convergence criteria were met (no improvement after 10 generations) or the maximum number of generations (100) was reached (default values in package rgenoud). Each generation corresponded to 1000 combinations of parameters. The optimized input parameters were recorded for building the model A. The peak-finding was performed by linearly correlating each point of the corrected spectra with the soil textural proportions. Then, the peak-finding selected the peaks near to the points whose correlation was higher than a given threshold. Peaks close to many emission lines were discarded because they could not be properly separated from the others. The elements were identified by using the NIST database

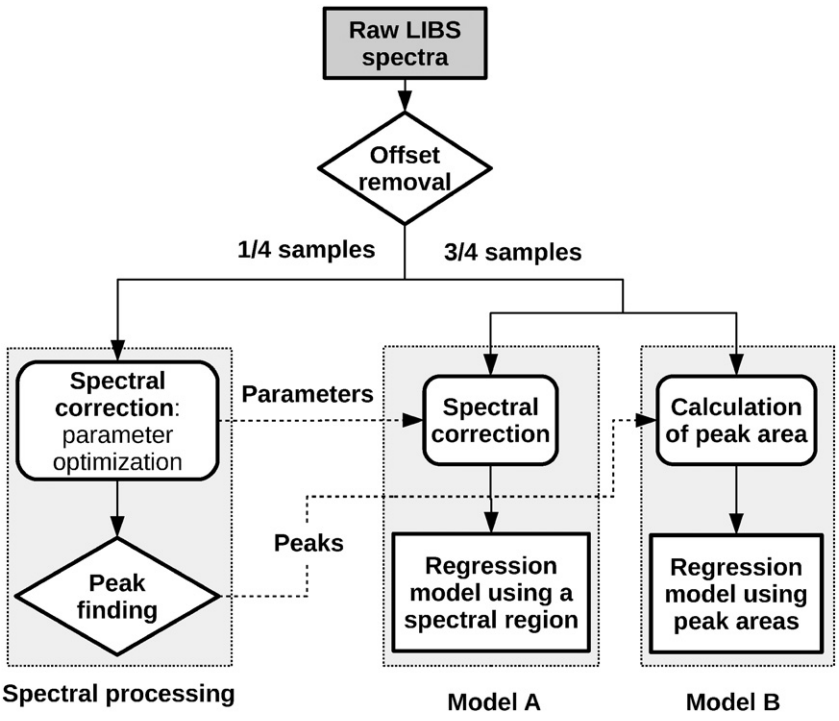

Fig. 1. Scheme used to process LIBS spectra and to create regression models for the estimation of the relative proportions of sand, clay, and silt in soils.

(Kramida et al., 2014). In this part of the analysis, the main idea was to find elements whose concentration varied according to the soil textural proportions. For instance, silicon concentration was expected to correlate positively with the relative proportion of sand in soil samples.

The third step in Fig. 1 was the process of building the regression models A and B: the first was based on the whole corrected spectra and the second on the peaks found in the previous step. Prior to building model A, the remaining spectra were corrected with the Savitzky–Golay filter and 4S Peak Filling method with the parameters optimized in the spectral processing part. Then, all spectra of each sample were averaged and used to build model A, which was tested by leave-one-out cross-validation, as in the spectral correction part.

Before the calculation of peak areas for the second model, a local baseline correction was used for each peak selected in the peak-finding step. Such a correction starts by choosing points in the left and right side of a peak, which only consist of random noise and without other peaks. Then, a linear function is fitted with the points chosen and used as a local baseline for the peak. The same procedure can be used for more than one peak in a small region provided that the points chosen for the correction are outside that region. This method is not suitable for large regions, since a straight line or a quadratic function may not be a good approximation for the baseline. This procedure was applied for all peaks identified in the peak-finding step, and the corresponding corrected regions were averaged for all spectra of each sample.

For each averaged spectrum, a Lorentzian distribution was then fitted for each peak in the spectral range selected. Model B was built using the area of the peaks as input variables for the PLSR method similarly to what was done for model A.

Since the PLSR model can use negative coefficients to correlate the spectral points with the variables *e* and *f*, the predicted textural proportions can also be negative, which has no physical meaning. In order to avoid such an inconsistency, all negative predictions were converted to zero, and the sum of predicted sand, silt, and clay proportions for each sample was normalized to 100%. After these corrections, the models were evaluated according to the Pearson correlation coefficient between the estimated and measured textural proportions and the root mean squared error (RMSE).

3. Results

The data were processed as in Fig. 1, starting with the offset removal and the sample division for the spectral correction and for building the models. The spectral correction consisted in optimizing the Savitzky–Golay filter to smooth the random noise and the 4S Peak Filling method to correct the baseline for each spectrometer region separately. The results of the optimization process were $\overline{\rho} = 0.83, 0.83, 0.82, 0.86, 0.87, 0.63,$ and 0.81 for spectrometers 1 to 7, respectively, and the parameters were recorded for building model A. Even though the baseline correction was optimized in relation to $\overline{\rho}$, a visual inspection was also performed to verify whether the baseline was physically meaningful, that is neither over-fitted nor above the spectrum (see example in Fig. 2(a)).

After the baseline correction, the peaks were found by using the linear correlation between the wavelength and the relative proportions of sand, silt, and clay, as in Fig. 2(b). Since most points were highly correlated with the textural proportions, we considered only those whose absolute correlation was higher than 0.80 with the proportions of sand, silt or clay. Also, to establish a model with a true physical-chemical meaning, regions of random noise, continuum background, and interfered lines were not considered, such as the regions 210.5–211.5 and 213.5–214.5 nm in Fig. 2(b). The Si I peak at 212.41 nm, on the other hand, was taken into account because of a correlation above 0.8 and higher than the neighborhood. The complete set of lines selected is shown in Table 1.

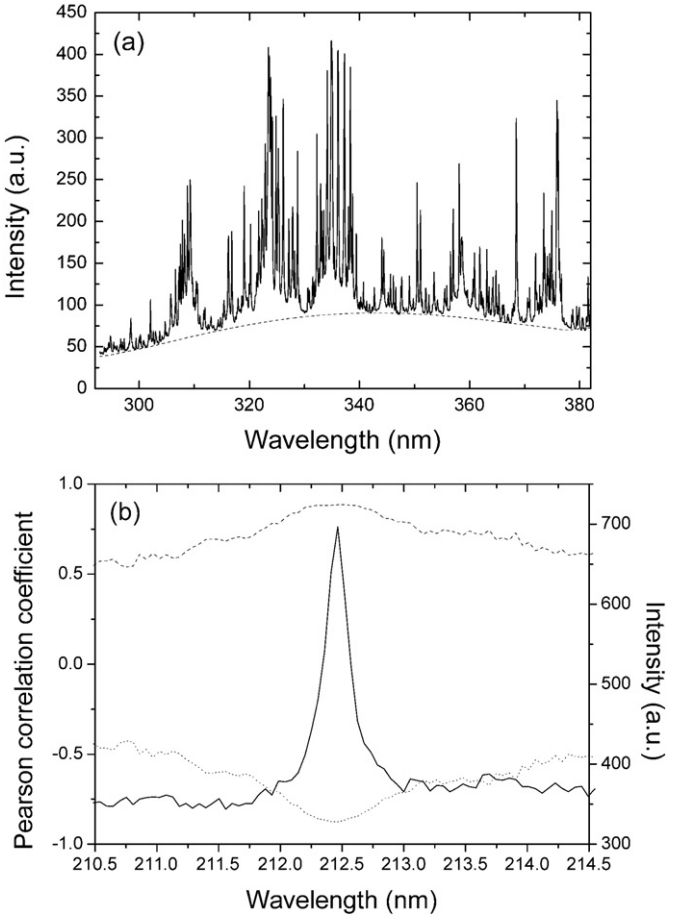

Fig. 2. (a) Example of a baseline estimated by 4S Peak Filling method (dashed line) in a LIBS spectrum (solid line). (b) Pearson correlation coefficient between the wavelength and the proportions of sand (dashed line) and clay (dot line). The solid line corresponds to a sample spectrum for the Si I peak at 212.41 nm.

The next step was the construction of the models, in which the PLSR method was used to correlate the textural proportions of the second set of samples with the spectral points of all spectrometer ranges and the areas of peaks of Table 1 for models A and B, respectively. For model A, the spectral baseline of all samples of the second set was corrected by using the Savitzky–Golay filter and 4S Peak Filling method

Table 1
Emission lines found in the peak-finding step and identified with NIST database (Kramida et al., 2014).

Wavelength (nm)			
Si I	**Fe I**	**Na I**	**Co II**
212.41	305.89	588.99	237.73
221.80	358.53	589.59	241.16
250.69	406.36	**Na II**	**Mg I**
251.61	432.57	288.42	285.21
288.16	438.35	520.85	**Mg II**
390.55	440.47	**Ca I**	279.55
Si II	528.36	610.27	279.49
412.08	532.41	612.22	280.27
413.09	532.80	**Ca II**	**V I**
634.56	544.69	866.21	412.35
636.99	**Fe II**	**K I**	**Ba I**
Ti I	233.27	766.49	553.54
394.86	235.53	769.89	**Ba II**
398.17	236.03	**Al I**	614.17
Ti II	238.86	308.21	**Be I**
306.62	242.41	394.40	235.08
454.96	244.45		

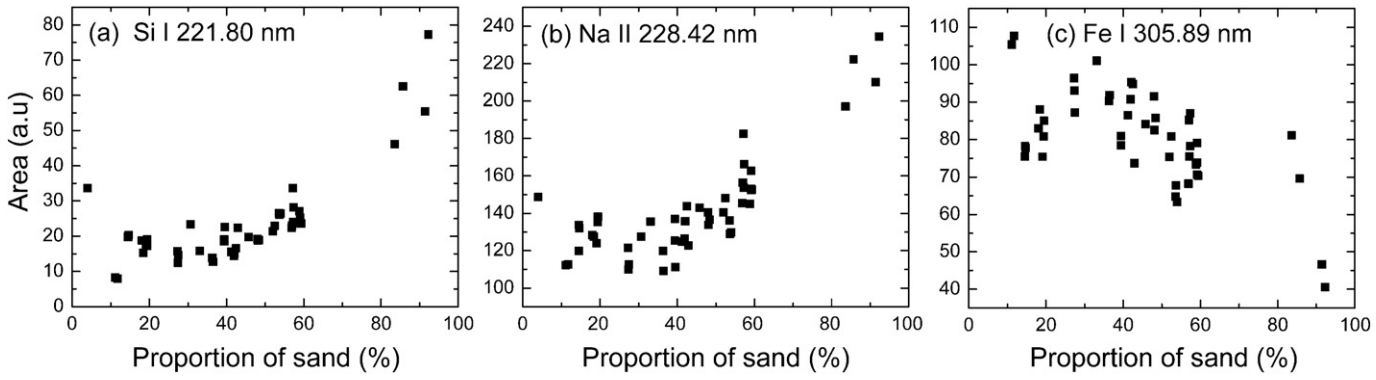

Fig. 3. Relation between the proportion of sand and the peak emission area of Si I at 221.80 nm (a), Na II at 228.42 nm (b), and Fe I 305.89 nm (c).

with the parameters determined in the optimization step of Fig. 1. Only then were the spectra of each sample averaged and used in the PLSR method.

For the second model, the areas of peaks in Table 1 were calculated for the spectra of all samples of the second set by fitting the Lorentz distribution after the local baseline correction, as described in Section 2.5. Before construction of the second model, the relation between the area of peaks and the textural proportions was analyzed to infer which elements were more abundant in each part. In particular, the concentration of Si and Na was positively correlated with the proportion of sand, in contrast to the concentration of Fe (Fig. 3).

The results of the leave-one-out cross-validation are shown in Fig. 4. The Pearson correlation coefficients for model A were 0.92, 0.85, and 0.90 with RMSE 8%, 4%, and 7% for sand (a), silt (b) and clay (c), respectively. On the other hand, the Pearson correlation coefficients for model B were 0.92, 0.86, and 0.91 with RMSE 8%, 4%, and 7% for sand (d), silt (e), and clay (f), respectively. Even though given in percentages, the uncertainties are absolute and not relative (i.e. the uncertainties represent

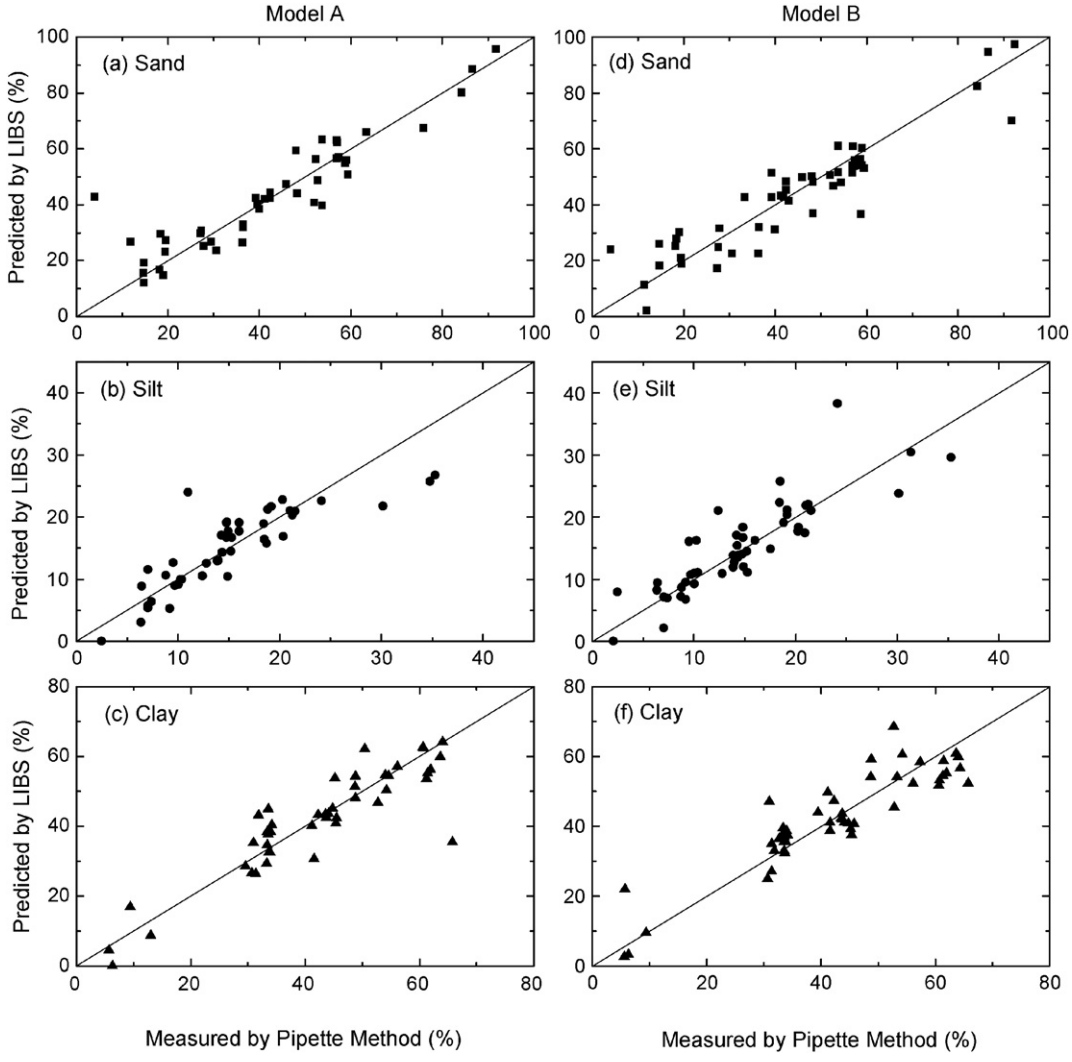

Fig. 4. Results of the leave-one-out cross-validation for models A and B and the relative proportions of sand, silt, and clay. The diagonal line represents the ideal calibration model.

percentage of sand, silt, or clay and are not relative to the textural proportions). Both models provided a strong correlation (higher than 0.85) with a RMSE below 8%. On average, the performance of model B was slightly better than that of model A: $\overline{\rho_B} = 0.90$ and $\overline{\rho_A} = 0.89$; $\overline{RMSE_B} = 6\%$ and $\overline{RMSE_A} = 6\%$.

The LIBS had a good agreement with the pipette method in terms of soil texture classification (Table 2). According to the soil texture triangle (Saxton et al., 1986), model B classified soil samples similarly to the pipette method, featuring 32 correct classifications. Of the misclassifications, 13 were classified into adjacent classes, whereas the other two were two and three classes distant.

4. Discussion

We found that LIBS can be used to estimate and classify soil texture based on the assumption of the chemical composition. Our results have shown that the relative textural proportions estimated by the calibration models were strongly correlated (higher than 0.85) with those measured by the pipette method. Such a correlation was achieved because of the relation between the relative textural proportions and the LIBS emission profile (both spectral range and peak areas) such as those in Fig. 2(b). Therefore, the elemental composition should differ between sand, silt, and clay particles. Similar conclusions were drawn for Martian soils, in which distinct compositions were found for coarse (>0.5 mm) and fine (<0.5 mm) particles (Cousin et al., 2015). In addition, Fig. 3 indicates that the proportion of sand is positively correlated with Si and Na peaks, but negatively with Fe peak. Similar observations for Si, Na, and Fe were also found in Martian soils (Cousin et al., 2015). Correlation of Si is not surprising since silica (SiO_2) is the most common constituent of sands; Na correlation may be related to the type of Brazilian rock from which sand is derived: probably feldspar, the composition of which includes Na. On the other hand, the negative correlation with Fe concentration may be because Fe oxides are mostly found in clay particles.

Models A and B provided a strong correlation coefficient with the proportions of sand, silt, and clay, but the latter performed better than the former. The slightly worse performance of model A may be explained by the fact that it includes all spectral points in the range from 188 to 980 nm, without excluding noise, baseline, and interfered peaks. In addition, it is more dependent on matrix effects than the second model, because fluctuations in the concentration of elements not included in Table 1 affect the calibration, in contrast to the second model.

Even though the spectral processing step did not completely remove the correlation with the background (Fig. 2(b)), it provided a means to

Table 2
Comparison of the percentages of sand, silt, and clay of the second sample set measured by the pipette method and estimated by LIBS and model B. The soil samples were classified according to Saxton et al. (1986) and considering only sand and clay percentages. The symbols * and † denote samples misclassified two and three classes distant, respectively.

	Reference values				Estimated by LIBS and model B			
Sample	Sand	Silt	Clay	Classification	Sand	Silt	Clay	Classification
1	27.3	18.4	54.3	Clay	17.2	22.3	60.4	Clay
2	39.9	18.9	41.2	Clay	31.2	19.1	49.7	Clay
3	57.2	9.2	33.6	Sandy clay loam	53.7	9.5	36.9	Sandy clay
4	27.8	16.0	56.2	Clay	31.5	16.2	52.3	Clay
5	92.3	2.1	5.6	Sand	97.4	0.0	2.6	Sand
6	36.5	14.8	48.7	Clay	32.0	14.0	54.0	Clay
7	59.4	6.4	34.2	Sandy clay loam	53.1	9.4	37.4	Sandy clay
8	57.1	9.2	33.7	Sandy clay loam	60.9	6.8	32.3	Sandy clay loam
9	48.2	9.5	42.3	Sandy clay	36.8	16.0	47.1	Clay
10	52.8	13.9	33.4	Sandy clay loam	46.7	13.8	39.5	Sandy clay
11	19.4	19.2	61.4	Clay	20.8	20.4	58.8	Clay
12	27.5	19.2	53.3	Clay	24.7	21.1	54.2	Clay
13	84.2	6.3	9.5	Loamy sand	82.4	8.2	9.4	Loamy sand
14	58.8	10.2	30.9	Sandy clay loam	36.8	16.2	47.1	Clay*
15	59.0	7.4	33.6	Sandy clay loam	60.2	6.9	33.0	Sandy clay loam
16	39.3	15.3	45.5	Clay	51.5	11.0	37.5	Sandy clay
17	52.0	14.4	33.6	Sandy clay loam	50.6	13.8	35.6	Sandy clay
18	48.3	10.1	41.6	Sandy clay	48.1	10.9	41.0	Sandy clay
19	19.0	20.3	60.7	Clay	30.1	18.4	51.6	Clay
20	36.3	14.8	48.8	Clay	22.5	18.3	59.2	Clay
21	4.0	30.2	65.8	Clay	23.9	23.8	52.3	Clay
22	14.7	20.9	64.4	Clay	26.0	17.4	56.5	Clay
23	18.4	20.2	61.3	Clay	27.9	17.7	54.4	Clay
24	33.3	13.9	52.8	Clay	42.7	11.9	45.5	Clay
25	18.2	21.0	60.7	Clay	25.1	21.8	53.1	Clay
26	41.2	15.2	43.6	Clay	43.2	14.4	42.3	Clay
27	56.9	12.4	30.7	Sandy clay loam	54.1	21.0	24.9	Sandy clay loam
28	86.6	7.1	6.4	Loamy sand	94.7	2.1	3.2	Sand
29	45.8	10.0	44.1	Sandy clay	49.7	9.2	41.0	Sandy clay
30	53.8	14.9	31.3	Sandy clay loam	61.0	12.0	27.0	Sandy clay loam
31	56.9	9.7	33.4	Sandy clay loam	51.5	10.7	37.8	Sandy clay
32	53.8	14.3	31.9	Sandy clay loam	51.6	15.4	33.0	Sandy clay loam
33	14.7	21.3	64.0	Clay	18.2	22.0	59.8	Clay
34	42.4	12.8	44.8	Clay	48.4	10.9	40.8	Sandy clay
35	48.1	10.4	41.6	Sandy clay	50.3	11.1	38.6	Sandy clay
36	42.4	14.0	43.7	Clay	45.2	12.7	42.0	Sandy clay
37	30.6	24.2	45.2	Clay	22.6	38.2	39.2	Clay loam
38	57.3	8.8	33.9	Sandy clay loam	56.0	8.6	35.4	Sandy clay
39	14.8	21.5	63.6	Clay	18.2	21.0	60.8	Clay
40	11.9	35.3	52.8	Clay	2.0	29.6	68.5	Clay
41	39.3	14.9	45.9	Clay	42.6	16.7	40.7	Clay
42	91.8	2.5	5.7	Sand	70.1	7.9	22.0	Sandy clay loam†
43	11.4	31.3	57.3	Clay	11.3	30.4	58.3	Clay
44	59.0	7.1	34.0	Sandy clay loam	54.1	7.1	38.8	Sandy clay
45	19.6	18.5	61.9	Clay	18.9	25.7	55.3	Clay

correct small LIBS spectral problems and to improve the estimation of soil texture. Also, the purpose of the peak-finding step was to find elements with strong correlation with the proportions of sand, silt, and clay. It was not an exhaustive search. Better algorithms to correct LIBS spectra and to find peaks are reserved for future works.

Despite the strong correlation with the reference technique, the uncertainties of the models (6%) were higher than those of the reference method (3%). Nonetheless, the purpose of this study was to show the possibility of estimating and classifying soil texture using LIBS and not to replace the reference technique. Even with such uncertainties, the LIBS can be useful in certain cases where time is crucial: for example, building a map of the soil texture for a large farm, an unfeasible task for the pipette method. Also, the precision of the reference method was low, providing uncertainties of 3%, 2%, and 3% for sand, clay, and silt, respectively. Precise values for textural soil proportions could have helped better identify the elements, which in turn could have reduced LIBS uncertainties.

Our results have shown that it is possible to estimate the proportions of sand, silt, and clay in terrain soils despite their complex composition. Our findings offer a new possibility to analyze not only chemical but also physical properties of soil samples. Therefore, LIBS is a powerful technique that can be used to estimate many soil properties in just a few minutes without chemical reagents.

5. Conclusions

We have shown that LIBS can be used to estimate the relative proportions of sand, silt, and clay in soil samples. We developed two models: one based on a range of 188 to 980 nm and the other based on emission lines of the elements Si, Na, Fe, Ti, Ca, K, Al, Co, Mg, V, Ba, and Be. We built the models with the PLSR method, taking into account the proportions of sand, silt, and clay of 60 Brazilian soil samples of varying composition. The results indicated that the models strongly correlated with the pipette method (Pearson correlation coefficient was higher than 0.85 for all textural proportions), meaning that LIBS can be used to estimate soil texture. Despite showing a higher uncertainty (6%) than that of the reference method (3%), the LIBS can be used for rapid scanning of the soil texture of large regions, which may be unfeasible by the pipette method. Since LIBS does not require sample preparation with chemical reagents, it is less error prone than the pipette method.

Our results could be improved with a more precise reference technique such as a gamma-ray attenuation analyzer, which may help identify other elements related to sand, silt, and clay content. Also, better algorithms to correct the spectra could help to find a higher number of peaks than that found in this work. Another way to improve our results would be to increase the number of samples by at least one order of magnitude (for instance 500 samples).

The procedure employed in this work can be extended to other soil chemical and physical properties. With models for several properties, LIBS can become a universal tool for soil analysis, including quantification of nutrients, organic matter, and contaminants, not only in the laboratory but also in situ.

Acknowledgments

The authors thank FAPESP (No. 06/61741-4) and EMBRAPA (No. 04.11.10.004.00.00) for the financial support of this study.

References

Bousquet, B., Sirven, J.B., Canioni, L., 2007. Towards quantitative laser-induced breakdown spectroscopy analysis of soil samples. Spectrochim. Acta B At. Spectrosc. 62, 1582–1589.

Braga, J.W.B., Trevizan, L.C., Nunes, L.C., Rufini, I.A., Santos D. Jr., Krug, F.J., 2010. Comparison of univariate and multivariate calibration for the determination of micronutrients in pellets of plant materials by laser induced breakdown spectrometry. Spectrochim. Acta B At. Spectrosc. 65, 66–74.

Brown, R.B., 2003. Soil Texture. Technical Report Fact Sheet SL-29. University of Florida. Soil and Water Science Department, Florida Cooperative Extensin Service, Institute of Food and Agricultural Sciences (http://edis.ifas.ufl.edu).

Chang, C.W., Laird, D.A., Mausbach, M.J., Hurburgh, C.R., 2001. Near-infrared reflectance spectroscopy—principal components regression analyses of soil properties. Soil Sci. Soc. Am. J. 65, 480–490.

Corsi, M., Cristoforetti, G., Hidalgo, M., Legnaioli, S., Palleschi, V., Salvetti, A., Tognoni, E., Vallebona, C., 2006. Double pulse, calibration-free laser-induced breakdown spectroscopy: a new technique for in situ standard-less analysis of polluted soils. Appl. Geochem. 21, 748–755.

Costa, L.F., Cesar Jr., R.M., 2001. Shape Analysis and Classification: Theory and Practice. CRC Press, Boca Raton, FL, USA.

Cousin, A., Meslin, P., Wiens, R., Rapin, W., Mangold, N., Fabre, C., Gasnault, O., Forni, O., Tokar, R., Ollila, A., Schröder, S., Lasue, J., Maurice, S., Sautter, V., Newsom, H., Vaniman, D., Mouélic, S.L., Dyar, D., Berger, G., Blaney, D., Nachon, M., Dromart, G., Lanza, N., Clark, B., Clegg, S., Goetz, W., Berger, J., Barraclough, B., Delapp, D., 2015. Compositions of coarse and fine particles in martian soils at gale: a window into the production of soils. Icarus 249, 22–42.

Cremers, D.A., Radziemski, L.J., 2006. Handbook of Laser-Induced Breakdown Spectroscopy. Wiley, Chichester, England.

Cremers, D.A., Ebinger, M.H., Breshears, D.D., Unkefer, P.J., Kammerdiener, S.A., Ferris, M.J., Catlett, K.M., Brown, J.R., 2001. Measuring total soil carbon with laser-induced breakdown spectroscopy (LIBS). J. Environ. Qual. 30, 2202–2206.

Curcio, D., Ciraolo, G., D'Asaro, F., Minacapilli, M., 2013. Prediction of soil texture distributions using vnir-swir reflectance spectroscopy. Procedia Environ. Sci. 19, 494–503.

Dawson, J.B., Snook, R.D., Price, W.J., 1993. Background and background correction in analytical atomic spectrometry. Part 1. Emission spectrometry. A tutorial review. J. Anal. At. Spectrom. 8, 517–537.

Ebinger, M.H., Harris, R.D., 2010. High resolution analysis of soil elements with laser-induced breakdown. US Patent 7,692,789.

Ebinger, M.H., Norfleet, M.L., Breshears, D.D., Cremers, D.A., Ferris, M.J., Unkefer, P.J., Lamb, M.S., Goddard, K.L., Meyer, C.W., 2003. Extending the applicability of laser-induced breakdown spectroscopy for total soil carbon measurement. Soil Sci. Soc. Am. J. 67, 1616–1619.

Ferreira, E.C., Ferreira, E.J., Villas-Boas, P.R., Senesi, G.S., Carvalho, C.M., Romano, R.A., Martin-Neto, L., Milori, D.M.B.P., 2014. Novel estimation of the humification degree of soil organic matter by laser-induced breakdown spectroscopy. Spectrochim. Acta B At. Spectrosc. 99, 76–81.

Ferreira, E.C., Milori, D.M.B.P., Ferreira, E.J., dos Santos, L.M., Martin-Neto, L., de Araújo Nogueira, A.R., 2011. Evaluation of laser induced breakdown spectroscopy for multielemental determination in soils under sewage sludge application. Talanta 85, 435–440.

Ferreira, E.C., Neto, J.A.G., Milori, D.M., Ferreira, E.J., Anzano, J.M., 2015. Laser-induced breakdown spectroscopy: extending its application to soil ph measurements. Spectrochim. Acta B At. Spectrosc. 110, 96–99.

Gee, G.W., Bauder, J.W., 1986. Particle-size analysis. In: Klute, A. (Ed.), Methods of Soil Analysis, Part 1, 2nd ed. American Society of Agronomy, Inc., Madison, WI, USA, pp. 383–411.

Harmon, R.S., De Lucia, F.C., Miziolek, A.W., McNesby, K.L., Walters, R.A., French, P.D., 2005. Laser-induced breakdown spectroscopy (LIBS) — an emerging field-portable sensor technology for real-time, in-situ geochemical and environmental analysis. Geochem. Explor. Environ. Anal. 5, 21–28.

Hassink, J., Bouwman, L., Zwart, K., Brussaard, L., 1993. Relationships between habitable pore space, soil biota and mineralization rates in grassland soils. Soil Biol. Biochem. 25, 47–55.

Hussain, T., Gondal, M.A., Yamani, Z.H., Baig, M.A., 2007. Measurement of nutrients in green house soil with laser induced breakdown spectroscopy. Environ. Monit. Assess. 124, 131–139.

Kettler, T.A., Doran, J.W., Gilbert, T.L., 2001. Simplified method for soil particle-size determination to accompany soil-quality analyses. Soil Sci. Soc. Am. J. 65, 849–852.

Kramida, A., Ralchenko, Y., Reader, J., NIST ASD Team, 2014. 2014. NIST Atomic Spectra Database (ver. 5.2)[Online]. National Institute of Standards and Technology, Gaithersburg, MD (Available at: http://physics.nist.gov/asd. Accessed: 2015–04–29).

Liland, K.H., 2015. 4S Peak Filling — baseline estimation by iterative mean suppression. MethodsX 2, 135–140.

Liland, K.H., Mevik, T.A.B.H., 2011. Optimal baseline correction for multivariate calibration using open-source software. Life Sci. Instrum. 3, 007.

Liland, K.H., Almøy, T., Mevik, B.H., 2010. Optimal choice of baseline correction for multivariate calibration of spectra. Appl. Spectrosc. 64, 1007–1016.

Madari, B.E., Reeves III, J.B., Machado, P.L.O.A., Guimarães, C.M., Torres, E., McCarty, G.W., 2006. Mid- and near-infrared spectroscopic assessment of soil compositional parameters and structural indices in two ferralsols. Geoderma 136, 245–259.

McCave, I.N., Syvitski, J.P.M., 2007. Principles and methods of geological particle size analysis. In: Syvitski, J.P.M. (Ed.), Principles, Methods, and Application of Particle Size Analysis. Cambridge University Press, New York, NY, USA, pp. 3–21.

Mebane Jr., W.R., Sekhon, J.S., 2011. Genetic optimization using derivatives: the rgenoud package for R. J. Stat. Softw. 42, 1–26.

Michel, A.P., Chave, A.D., 2007. Analysis of laser-induced breakdown spectroscopy spectra: the case for extreme value statistics. Spectrochim. Acta B At. Spectrosc. 62, 1370–1378.

Miziolek, A., Palleschi, V., Schechter, I., 2006. Laser-Induced Breakdown Spectroscopy (LIBS): Fundamentals and Applications. Cambridge University Press, New York, NY, USA.

Naime, J.M., Vaz, C.M.P., Macedo, A., 2001. Automated soil particle size analyzer based on gamma-ray attenuation. Comput. Electron. Agric. 31, 295–304.

Nicolodelli, G., Marangoni, B.S., Cabral, J.S., Villas-Boas, P.R., Senesi, G.S., dos Santos, C.H., Romano, R.A., Segnini, A., Lucas, Y., Montes, C.R., Milori, D.M.B.P., 2014. Quantification

of total carbon in soil using laser-induced breakdown spectroscopy: a method to correct interference lines. Appl. Opt. 53, 2170–2176.
Palanco, S., López-Moreno, C., Laserna, J.J., 2006. Design, construction and assessment of a field-deployable laser-induced breakdown spectrometer for remote elemental sensing. Spectrochim. Acta B At. Spectrosc. 61, 88–95.
Pontes, M., Cortez, J., Galvão, R., Pasquini, C., Araújo, M., Coelho, R., Chiba, M., De Abreu, M., Madari, B., 2009. Classification of Brazilian soils by using LIBS and variable selection in the wavelet domain. Anal. Chim. Acta 642, 12–18.
R Core Team, 2014. R: A Language and Environment for Statistical Computing. R Foundation for Statistical Computing, Vienna, Austria (URL: http://www.R-project.org).
Rossel, R.A.V., Walvoort, D.J.J., McBratney, A.B., Janik, L.J., Skjemstad, J.O., 2006. Visible, near infrared, mid infrared or combined diffuse reflectance spectroscopy for simultaneous assessment of various soil properties. Geoderma 131, 59–75.
Savitzky, A., Golay, M.J., 1964. Smoothing and differentiation of data by simplified least squares procedures. Anal. Chem. 36, 1627–1639.
Saxton, K., Rawls, W., Romberger, J., Papendick, R., 1986. Estimating generalized soil-water characteristics from texture. Soil Sci. Soc. Am. J. 50, 1031–1036.
Senesi, G., Dell'Aglio, M., Gaudiuso, R., De Giacomo, A., Zaccone, C., De Pascale, O., Miano, T., Capitelli, M., 2009. Heavy metal concentrations in soils as determined by laser-induced breakdown spectroscopy (LIBS), with special emphasis on chromium. Environ. Res. 109, 413–420.
Silva, R.M., Milori, D.M.B.P., Ferreira, E.C., Ferreira, E.J., Krug, F.J., Martin-Neto, L., 2008. Total carbon measurement in whole tropical soil sample. Spectrochim. Acta B At. Spectrosc. 63, 1221–1224.
Singh, J.P., Thakur, S.N., 2007. Laser-Induced Breakdown Spectroscopy. Elsevier Science, Amsterdam.
Taubner, H., Roth, B., Tippkötter, R., 2009. Determination of soil texture: comparison of the sedimentation method and the laser-diffraction analysis. J. Plant Nutr. Soil Sci. 172, 161–171.
Theriault, G.A., Bodensteiner, S., Lieberman, S.H., 1998. A real-time fiber-optic LIBS probe for the in situ delineation of metals in soils. Field Anal. Chem. Technol. 2, 117–125.
Tobias, R.D., 1995. An introduction to partial least squares regression. Proc. Ann. SAS Users Group Int. Conf., 20th, Orlando, FL, pp. 2–5.
Tognoni, E., Cristoforetti, G., Legnaioli, S., Palleschi, V., 2010. Calibration-free laser-induced breakdown spectroscopy: state of the art. Spectrochim. Acta B At. Spectrosc. 65, 1–14.
Wold, S., Sjöström, M., Eriksson, L., 2001. PLS-regression: a basic tool of chemometrics. Chemom. Intell. Lab. Syst. 58, 109–130.